Spatiotemporal Vortex Matter Oscillations in $Bi_2Sr_2CaCu_2O_{8+\delta}$ Crystals

B. Kalisky,[1,*] M. Gitterman,[1] B. Ya. Shapiro,[1] I. Shapiro,[1] A. Shaulov,[1] T. Tamegai,[2] and Y. Yeshurun[1]

[1]*Institute for Superconductivity, Department of Physics, Bar-Ilan University, Ramat-Gan, 52900 Israel*

[2]*Department of Applied Physics, The University of Tokyo, Hongo, Bunkyo-ku, Tokyo 113-8656, Japan*

(Received 2 July 2006; published 4 January 2007)

We observed an oscillatory behavior, both in space and time, of the induction in $Bi_2Sr_2CaCu_2O_{8+\delta}$ crystals exposed to a steady magnetic field. This new "flux waves" phenomenon appears near the order-disorder vortex phase transition, under specific conditions of temperature and induction gradient. A theoretical description of this effect is based on two coupled equations: the Landau-Khalatnikov dynamic equation for the order parameter of the vortex phase transition and the diffusion equation for the time evolution of the magnetic induction. A linear stability analysis of these equations predicts an oscillatory instability characterized by a period and wavelength in accordance with the experimental results.

DOI: 10.1103/PhysRevLett.98.017001 PACS numbers: 74.25.Qt, 64.60.Cn, 74.72.Hs

Extensive efforts have been made in the study of spatiotemporal pattern formation in nonequilibrium systems (see Ref. [1], and references therein). Such patterns are encountered in hydrodynamics [2], nonlinear optics [3], solid-state physics [4], chemistry [5], and biology [6]. All of these systems involve nonlinear diffusion processes in dissipative media. A linear stability analysis of the equations describing these processes, predicts instabilities oscillating in space and/or time. In this article we show, for the first time, an oscillating pattern in the vortex matter of high-temperature superconductors, spontaneously generated in the absence of external ac magnetic field. Our observation of a quasiperiodic pattern of the magnetic induction, both in time and space, is unique, as normally one observes a monotonic time decay of the magnetic induction in superconductors under steady fields [7,8]. The oscillatory behavior, referred here as "flux waves" [9], is observed near the vortex order-disorder phase transition [10], under specific conditions of temperature and induction gradient.

Flux waves were observed in a series of $Bi_2Sr_2CaCu_2O_{8+\delta}$ (BSCCO) single crystals grown by using the floating zone method [11]. These crystals commonly have narrow stripelike defects extending parallel to the crystallographic a axis; the origin of these defects is still debated [12]. Here we report on measurements performed on a $1.4 \times 8 \times 0.05$ mm^3 crystal ($T_c \sim 92$ K) in which the vortex order-disorder transition occurs at $B_{od} \approx$ 400–450 G [13]. The stripelike defect in this crystal runs parallel to the long edge, at a distance of $\sim$350 μm. After zero-field-cooling the sample to the target temperature, the sample was exposed to an external magnetic field parallel to the crystallographic c axis, raised abruptly to a target value between 140 and 840 Oe with rise-time $<$25 ms. Immediately after reaching the target field, magneto-optical [14] snapshots of the induction distribution across the sample surface were recorded at time intervals of 40 ms for 5.5 s, using an iron-garnet indicator with in-plane anisotropy and a high speed CCD camera.

Figure 1(a) exhibits induction profiles, magneto-optically measured across the sample at various times after application of 430 G at 24 K. As described previously [15], exposure of the sample to an external magnetic field lower than B_{od} creates a metastable disordered vortex states characterized by relatively large current density J. This is

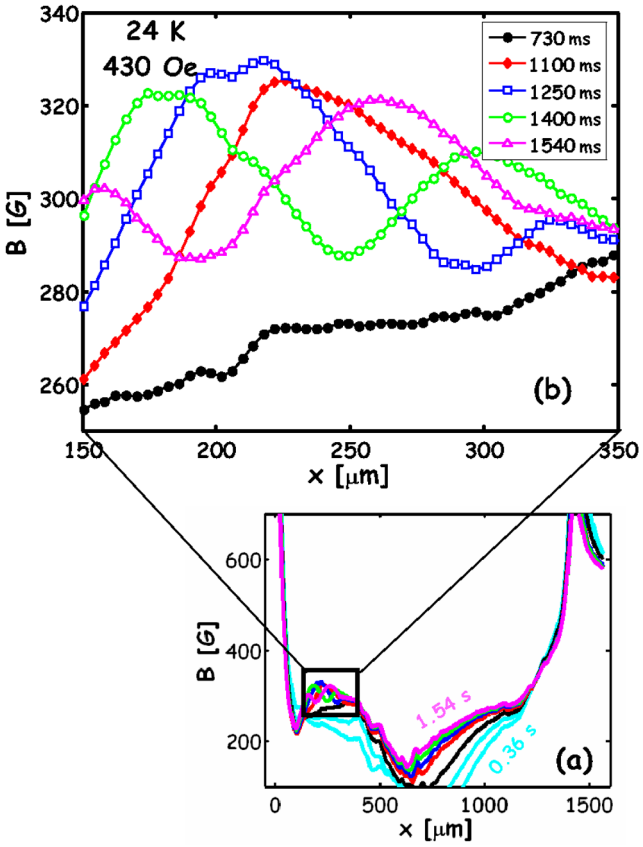

FIG. 1 (color online). (a) Induction profiles across the sample at various times between 0.3 and 1.5 s after application of $H =$ 430 Oe at 24 K. The square marks the region which is enlarged in (b).

signified by the Bean-like profiles which are initially ($t \leq 0.6$ s) observed. This metastable vortex state is subsequently annealed at a rate which strongly depends on the proximity of the induction B to B_{od}; the annealing rate rapidly decreases as B approaches B_{od} [13]. The figure clearly shows fast annealing of the injected disordered state on the left hand side of the sample ($x < 350$ μm); this is evident from the dome-shape profile, signifying a low-J ordered vortex state [16] that is quickly reached in this region. In contrast, for $x > 350$ μm, Bean profiles persist during the time window of the experiment. These results suggest the presence of two regions in the sample (regions L and R) characterized by a larger B_{od} left to the stripe (region L). The stripe defect is, presumably, the border between these two regions.

As time evolves, an unstable oscillating pattern is developed, as shown in Fig. 1(b) which zooms on the induction profiles of Fig. 1(a) at the indicated region. It is important to note that the oscillating pattern appears approximately 1 s after the application of the external field, i.e., long time after the external field stabilizes (less than 25 ms). The wave pattern exhibits a wavelength and amplitude of approximately 130 μm and 40 G, respectively. During the whole process vortices creep into the sample due to regular relaxation after application of an external magnetic field; we note that the waves move in the opposite direction to the incoming flux from the edge of the sample. For observation of the full time evolution of the oscillatory induction profiles, the reader is referred to our Web site [17].

In addition to the spatial oscillation described above, the data exhibit oscillations in time, as demonstrated in Fig. 2. For example, at 24 K, for applied field of 430 Oe, the magnetic induction B is oscillatory with time, with a period of ≈ 0.75 s. These oscillations are observed in a limited range of external fields and their period pronouncedly decreases with temperature. The temperature dependence of the period is described in the main panel of Fig. 3, exhibiting an exponential decrease of the period as the temperature increases.

The inset to Fig. 3 describes the oscillations amplitude as a function of the external magnetic field. The amplitude exhibits a nonmonotonic dependence on the external field H, with a maximum around $H = 420$ Oe. The fast decay of the amplitude on both sides of the maximum indicates that the oscillatory behavior occurs only in the vicinity of B_{od}. This implies that the oscillations are associated with the vortex order-disorder phase transition.

The experimental results described above imply that the nearly flat induction profile (low-J phase) near the vortex order-disorder transition line is unstable, giving rise to the evolution of oscillatory behavior of the induction in space and time. In our experiment, the condition of a nearly flat profile is fulfilled left to the stripe defect.

In the following we outline a theoretical analysis, showing that under these conditions (proximity to the order-disorder transition and a nearly flat profile) an oscillatory instability can be created in the vortex matter. In the theory we distinguish between the ordered and disordered vortex phases by means of an order parameter Ψ, defined in a way analogous to the order parameter in solid-state order-disorder transition [18]: $\Psi = 0$ and $\Psi = \Psi_0(B)$ for the disordered and ordered vortex phases, respectively. The annealing of the injected metastable disordered state ($\Psi = 0$) toward the thermodynamic ordered phase ($\Psi = \text{const}$) is described by the Landau-Khalatnikov dynamic equation [19]:

$$\frac{\partial \Psi}{\partial t} = -\Gamma \frac{\delta F}{\delta \Psi}, \tag{1}$$

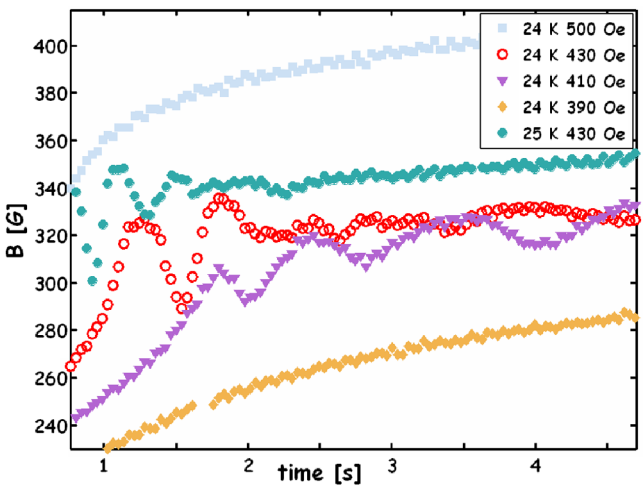

FIG. 2 (color online). Time dependence of local induction B measured at $x = 240$ μm after abrupt application of the indicated external magnetic field.

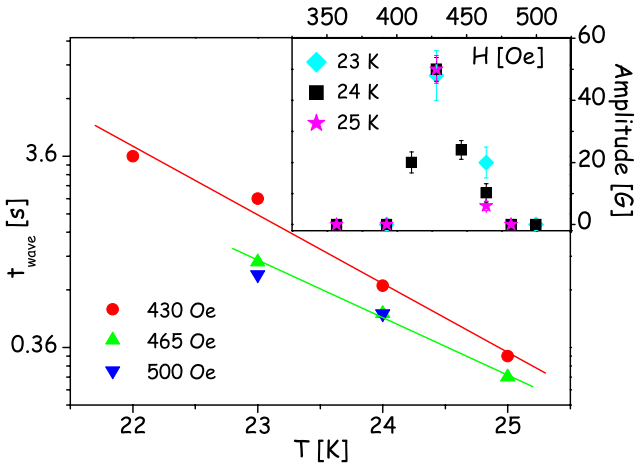

FIG. 3 (color online). The period of the "flux waves" as a function of temperature for different applied fields. Lines are linear fits. Inset: the amplitude of the oscillations as a function of H for different temperatures.

where $F = 1/2 \int [D(\partial\Psi)^2 - \alpha\Psi^2 + \gamma_0\Psi^4/2]\, d^3r$ is the free energy, Γ is the relaxation constant, and $\alpha = \alpha_0(1 - B/B_{\rm od})$, D, and γ_0 are the Landau expansion coefficients for the field-driven order-disorder vortex phase transition. The relaxation of B is governed by a nonlinear diffusion equation $\partial B/\partial t = -c\partial E/\partial x$ where $E = R_F J \exp(-U/kT)$ is the electric field, $R_F = R_n(B/B_{c2})$ is the flux flow resistivity, and U is the pinning potential. Assuming a logarithmic dependence of U on the current J [20]: $U = U_0 \ln(J_c/J)$, where J_c is the critical current density, one obtains [7]:

$$\frac{\partial B}{\partial t} = \frac{c^2}{4\pi}\frac{\partial}{\partial x}\left[D_f \frac{\partial B}{\partial x}\right]; \qquad D_f = R_F\left(\frac{J}{J_c[\Psi]}\right)^{\sigma}, \quad (2)$$

where D_f is the diffusion coefficient for flux creep, and $\sigma = U_0/T$. Experimentally [21], J_c increases in the transition from the ordered to the disordered vortex phase. We assume that $J_c[\Psi]$ is an analytical function which decreases from a large value in the disordered vortex phase, to a smaller value J_{c0}, in the ordered vortex phase. We note that the results of the linear stability analysis are rather general and do not depend on the explicit form of the function $J_c[\Psi]$. Our only requirement is that the critical currents (and hence the vortex diffusion coefficients), are different in the ordered and disordered vortex phases. Clearly, Eqs. (1) and (2), when treated separately, describe a monotonous relaxation of Ψ and B, respectively, toward their equilibrium values. However, considering the coupling of these equations through $J_c = J_c[\Psi]$, our analysis shows that under certain conditions, an oscillatory behavior of the induction B is obtained.

The following scenario provides an intuitive description of this phenomenon. As mentioned above, exposing the sample to an external field is followed by injection of a metastable disordered vortex state ($\Psi = 0$) into the sample. The generation of a dome-shaped profile in region L indicates a fast annealing, governed by Eq. (1), of the disordered state in this region, toward the thermodynamic ordered state. Consequently, J_c in this region decreases, causing an increase in the diffusion coefficient $D_f \propto 1/J_c$; see Eq. (2). On the other hand, in region R, a disordered metastable state persists, indicated by the Bean profiles, maintaining a large J_c and thus relatively low diffusion coefficient D_f. The gradient in the diffusion coefficient at the interface between these two regions causes an accumulation of vortices at the interface up to a point where an inverted slope of B is created. The accumulation process comes to a halt because the increase in B is followed by a decrease in Ψ which, in turn, causes an increase in J_c and a decrease in D_f. The inverted slope of $B(x)$ serves as a driving force for flux motion in the opposite direction, toward the sample edge where B is smaller. As a result of the smaller B, the annealing of Ψ described by Eq. (1) dominates again, bringing the system back to an ordered state with low J_c and large D_f, and the process repeats itself. Note, however, that after each cycle B increases and, as a result, the annealing process is becoming less and less effective, and therefore the oscillations decay.

A detailed theoretical analysis of the coupled equations (1) and (2) will be described elsewhere. In essence, a linear stability analysis of these equations leads to an oscillatory dynamics similar to that described in Ref. [5]. In the analysis we assume an almost flat profile of induction B_0 between $x = 0$ and d, such that $(B_{\rm od} - B_0) \gg (dB/dx)d$, resulting in approximately a constant slope J_0. Note that these assumptions are fulfilled in the experiment, referring to the lower profile of Fig. 1 that signifies the beginning of the instability. We present Ψ and B in the form $\Psi = \Psi_0 + \phi e^{iqx+\Omega t}$; $B = B_0 + be^{iqx+\Omega t}$, where b and ϕ are the amplitudes of the perturbations characterized by a wave number q and a frequency Ω. Linearizing Eqs. (1) and (2), one obtains $\Omega(q)$ as a solution of the equation

$$(iQF_3 - Q^2F_2 - \omega)(Q^2\nu_1 + \varepsilon + \omega) - i\nu_3 Q = 0, \quad (3)$$

$\omega = \Omega\tau$, $Q = qcB_{\rm od}/4\pi J_{c0}$, $\varepsilon = 2(1 - \bar{b})$, $\bar{b} = B_0/B_{\rm od}$, $\tau = 4\pi R_n J_{c0}^2/B_{\rm od}B_{c2}$, $F_3 = j_0|j_0|^{\sigma}$, $j_0 = J_0/J_{c0}$, $F_2 = (\sigma + 1)\bar{b}|j_0|^{\sigma}$, $\nu_1 = 4\pi\Gamma D B_{c2}/c^2 R_n B_{\rm od}$, $\nu_3 = f_1\bar{b}F_3\alpha_0^{3/2}\Gamma\tau/\gamma_0^{1/2}$, $f_1 \approx |\partial \ln J_c/\partial \ln\Psi_0|$.

Figure 4 shows the real and imaginary part of $\Omega(q)$ for $\alpha_0\Gamma = 10$ Hz [18], $\varepsilon = 0.2$, and $J_0 = 0.1$ G/μm. The behavior of Re(Ω) in Fig. 4 is characteristic of the Turing-type instability [22]. The range of q for which Re(Ω) > 0 and Im(Ω) $\neq 0$ is the instability regime, characterized by oscillations in time and space with growing amplitude. This is typical of Zhabotinsky-Belousov dynamics [5] where the time-independent steady state solution is not established; instead, the system exhibits oscillatory behavior. Referring to Fig. 4, the most unstable

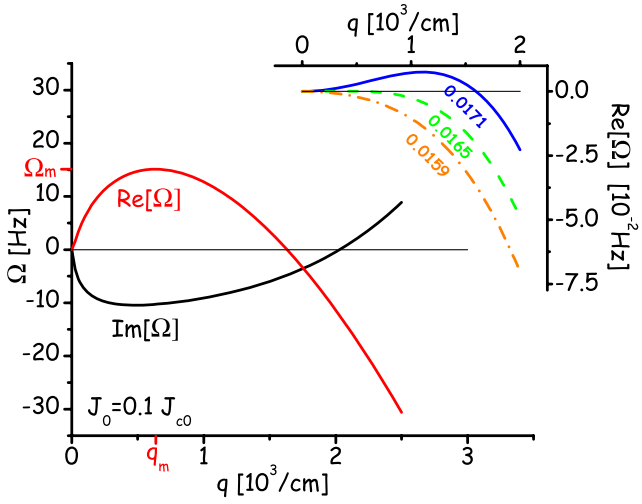

FIG. 4 (color online). Calculated real and imaginary parts of $\Omega(q)$. Inset: Re[$\Omega(q)$] for different values of the steady induction gradient (in units of J_{c0}).

mode is characterized by a wave number q_m corresponding to the maximum in $\mathrm{Re}(\Omega)$ and by an oscillation frequency Ω_m corresponding to the $\mathrm{Im}(\Omega)$ at q_m. The inset to Fig. 4 shows $\mathrm{Re}[\Omega(q)]$ for different J_0. As one can see, the instability [i.e., positive $\mathrm{Re}[\Omega(q)]$] appears above some threshold slope $J_0 \approx 0.016 J_{c0}$.

We discuss now the experimental results in view of the theory outlined above. The instability frequency can be predicted by using typical values for the parameters: $J_{c0} = 10^5$ A/cm^2, $\sigma = 2.5$, $B_{\mathrm{od}} = 400$ Oe, $R_n = 10^{-4}\ \Omega \cdot \mathrm{cm}$, and $B_{c2} = 10^7$ Oe. One obtains $\Omega_m \cong 1$ Hz, and $q_m = 800\ \mathrm{cm}^{-1}$, in reasonable agreement with the experimental data. q_m and Ω_m are sensitive to both induction and temperature. The calculated characteristic period of the oscillations is $t_0 \simeq [\mathrm{Im}(\Omega)]^{-1} \propto (1 - B/B_{\mathrm{od}})^{-1/3}(J_{c0}/J_0)^{(2\sigma+2)/3}$. Assuming [7,23]: $J_{c0} \propto \exp[-T/T_0(B)]$, where T_0 is the temperature limiting the single vortex pinning regime, one obtains $t_0 \propto \exp[-(2\sigma + 2)/3T/T_0(B)]$. This exponential decrease of the period with temperature is in good agreement with the experimental data shown in Fig. 2. The temperature dependence of the wavelength can also be compared to the theoretical predictions. However, as expected theoretically, we find only weak dependence of the wavelength on temperature which cannot accurately be resolved taking into account the large error bars.

In conclusion, we discovered a new phenomenon of flux waves, spontaneously generated in BSCCO under a steady magnetic field. It should be noted that previous reports on flux waves in $YBa_2Cu_3O_{7-\delta}$ referred to a fundamentally different flux motion, generated by a periodic external magnetic field [9]. In our experiment, the flux waves are spontaneously generated near the order-disorder vortex phase transition line, either by tuning the field at a constant temperature as reported here, or by tuning temperature at a constant field as will be reported elsewhere. We outlined a theory which describes this phenomenon, yielding good agreement with the experimentally measured wavelength and period of the oscillations.

We acknowledge important discussions with D. Kessler and E. Zeldov. This research was supported by the Israel Science Foundation (Grants Nos. 8003/02 and 4/03-11.7), Heinrich Hertz Minerva Center for High Temperature Superconductivity, and the German-Israel Foundation. T. T. acknowledges support from a grant-in-aid for scientific research from the Ministry of Education, Culture, Sports, Science and Technology.

*Present address: Department of Condensed Matter Physics, Weizmann Institute, 76100 Rehovot, Israel. Electronic address: beena.kalisky@weizmann.ac.il

[1] M. C. Cross and P. C. Hohenberg, Rev. Mod. Phys. **65**, 851 (1993).
[2] S. Chandrasekhar, *Hydrodynamics and Hydromagnetic Stability* (Clarendon Press, Oxford, 1961).
[3] J. V. Moloney and A. C. Newell, Physica (Amsterdam) **44D**, 1 (1990).
[4] D. A. Kessler, J. Koplik, and H. Levine, Adv. Phys. **37**, 255 (1988).
[5] A. M. Zhabotinsky, in *Oscillations and Traveling Waves in Chemical Systems*, edited by R. J. Field and M. Burger (Wiley & Sons, New York, 1985).
[6] K. Kurin-Csörgei *et al.*, J. Phys. Chem. **100**, 5393 (1996).
[7] G. Blatter *et al.*, Rev. Mod. Phys. **66**, 1125 (1994).
[8] For a review, see Y. Yeshurun, A. P. Malozemoff, and A. Shaulov, Rev. Mod. Phys. **68**, 911 (1996).
[9] M. V. Indenbom *et al.*, Nature (London) **385**, 702 (1997).
[10] T. Giamarchi and P. LeDoussal, Phys. Rev. Lett. **72**, 1530 (1994); V. Vinokur *et al.*, Physica (Amsterdam) **295C**, 209 (1998).
[11] N. Motohira *et al.*, J. Ceram. Soc. Jpn. **97**, 1009 (1989).
[12] M. Yasugaki *et al.*, Phys. Rev. B **67**, 104504 (2003); I. F. Tsu *et al.*, Physica (Amsterdam) **349C**, 8 (2001); R. Gerbaldo *et al.*, Physica (Amsterdam) **354C**, 173 (2001); L. Gozzelino *et al.*, Int. J. Mod. Phys. B **17**, 879 (2003); M. Li *et al.*, Physica (Amsterdam) **408C**, 25 (2004).
[13] B. Kalisky *et al.*, Phys. Rev. B **68**, 224515 (2003).
[14] For recent reviews, see *Magneto-Optical Imaging*, edited by T. H. Johansen and D. V. Shantsev, NATO Science Series II: Mathematics, Physics and Chemistry Vol. 142 (Kluwer Academic Publishers, Dordrecht, 2004); in Proceedings of the First NATO Advanced Research Workshop on Magneto-Optical Imaging, Oystese, Norway, 2003.
[15] D. Giller *et al.*, Phys. Rev. Lett. **84**, 3698 (2000).
[16] E. Zeldov *et al.*, Phys. Rev. Lett. **73**, 1428 (1994).
[17] Electronic address: http://www.biu.ac.il/ESC/htslab/beena/waves/.
[18] D. Giller *et al.*, Phys. Rev. B **63**, 220502 (2001).
[19] L. D. Landau and I. M. Khalatnikov, in *The Collected Works of L. D. Landau*, edited by D. ter Haar (Pergamon, Oxford, 1965), pp. 626–633. The noise term may be ignored in linear stability analysis of this equation.
[20] E. Zeldov *et al.*, Appl. Phys. Lett. **56**, 680 (1990).
[21] See, e.g., M. Daeumling, J. M. Seuntjens, and D. C. Larbalestier, Nature (London) **346**, 332 (1990).
[22] A. M. Turing, Phil. Trans. R. Soc. B **237**, 37 (1952).
[23] An exponential decrease of $J_c(T)$ in BSCCO is a good approximation for the measured J_c; see e.g. V. V. Moshchalkov *et al.*, Phys. Rev. B **50**, 639 (1994).